Title

LIMITATION TO SIGNIFICANT INFORMATION IN BIOLOGICAL ELECTRON MICROSCOPY AS A RESULT OF RADIATION DAMAGE.

Author

Glaeser, Robert M.

Publication Date

1970-10-01

Submitted to Ultrastructural Research

UCRL-20167
Preprint

LIMITATION TO SIGNIFICANT INFORMATION IN BIOLOGICAL ELECTRON MICROSCOPY AS A RESULT OF RADIATION DAMAGE

Robert M. Glaeser

October 1970

AEC Contract No. W-7405-eng-48

LAWRENCE RADIATION LABORATORY
UNIVERSITY of CALIFORNIA BERKELEY

DISCLAIMER

LIMITATIONS TO SIGNIFICANT INFORMATION IN BIOLOGICAL ELECTRON MICROSCOPY AS A RESULT OF RADIATION DAMAGE.[1]

Robert M. Glaeser, Division of Medical Physics and Donner Laboratory, University of California, Berkeley, California 94720.

Running Title: "RADIATION DAMAGE"

---

1. Preliminary reports of portions of this work have been presented at the 7th International Congress of Electron Microscopy (12) and at the 28th Annual Meeting of the Electron Microscopy Society of America (11).

Abstract

Quantitative measurements of radiation damage in crystalline specimens of l-valine, adenosine, and catalase (uranyl acetate stained) have been made by observing the loss of the electron diffraction pattern. Reciprocity of specimen lifetime and current density at the specimen demonstrates the absence of any dose-rate effect, such as specimen heating, as a cause of specimen damage. Specimen lifetimes at high voltages are about two and a half times greater than at conventional voltages, and it is shown that this is consistent with the dependence of linear energy loss upon accelerating voltage. The limiting resolution for meaningful observation is considered in terms of the statistics of observation at particle fluxes that are specified from the specimen lifetime data. The best values are probably not better than 50 Å for l-valine, 20 Å for adenosine, and 15 Å for catalase.

Introduction

Numerical image-processing techniques recently introduced into biological electron microscopy suggest that electron microscopy could be developed into a method equivalent to or even superior to x-ray crystallography for three-dimensional structure analysis (17). The Fourier projection theorem was first used by DeRosier and Klug, for a structure with helical symmetry (5). The method has since been extended by Crowther et al. to a non-helical structure (4). Solution of simultaneous linear equations in real space (the projection matrix method) has been employed by Hart (15) and by Vainshtein (36). Continuing improvements in instrumental resolving power lend hope to the expectation that useful three-dimensional structural information can be obtained at resolutions better than 5 Å. Application of transfer function theory in electron microscopy (8, 18, 33, 38) suggests that numerical processing of electron micrographs can compensate for systematic errors due to instrumental defects. Phase distortion and translational (vibrational) blurring are the most serious defects at high resolution. It is well known that improved specimen preparation methods are needed for biological materials in order to take advantage at high resolution of the powerful synthesis of the mathematics of signal theory and of crystallography. It is also apparent that radiation damage limits the usefulness of electron microscope data, regardless of the initial quality of the specimen. The purpose of the work reported here is to quantitatively estimate the resolution to which useful structural information might be obtained for representative biological materials.

The difficulty of obtaining high resolution lattice images of organic molecular crystals indicates that radiation damage limits the meaningful resolution that might be obtained with biological specimens. The phthalocyanines, which like the porphyrins may be expected to be extraordinarily resistant to bond-damage subsequent to ionization by radiation (26), are in most instances suitable only for producing lattice images to a resolution of about 10 Å (23). A more complicated crystal-image structure having a resolution of ~5 Å has been reported for the particular derivative Cu-hexadecachlorophthalocyanine (35). By comparison lattice resolutions of 3.35 Å and better are obtainable with graphitized carbon (41), and a lattice resolution of 0.88 Å has been obtained with crystalline nickel (42). These examples emphasize that specimen radiation damage rather than the instrumental resolving power or the experimental technique of the microscopist is the limiting factor in obtaining high resolution images of crystals of biological molecules.

The question of radiation damage has received an excellent analysis and review in the recent paper of Stenn and Bahr (30). These authors suggest that radiation damage might not affect the meaningful information except at resolutions of less than 4 Å. This estimate may be valid in special cases such as are mentioned later in the discussion, but the data presented here indicates that radiation damage can often limit the meaningful resolution to 15 Å - 20 Å or more. It is possible, however, that new experimental methods can reduce the apparent effect of radiation damage.

A direct measurement of the degree of radiation damage and of the variation in radiation sensitivity for different crystalline biological

materials can be obtained by observing the radiation dose that causes the fading of the electron diffraction pattern to a chosen end point (20, 32). Data are presented here for the radiation sensitivity of l-valine, adenosine, and uranyl-acetate-stained catalase. The limiting effect of radiation damage upon image resolution can be calculated from equations that take into account the contrast that is available at that resolution, the radiation-induced yield for bond damage, and other relevant parameters.

Materials

Crystals of l-valine and of adenosine were grown from aqueous solution by evaporation of solvent at room temperature. A small drop of solution was placed directly upon a formvar-coated specimen grid. The drop size and solution concentration both influence the crystal thickness and the number of crystals. The optimal conditions are best found by empirical trial.

Commercial preparations of bovine liver catalase (C.F. Boehringer & Soehne, Mannheim) were recrystallized by the method of Wrigley (40). In this method a solution of catalase in 11% NaCl is dialized against decreasing concentrations of phosphate buffer at pH 6.3, ending either with 0.001 M buffer or with distilled water. Specimens were mounted on formvar coated grids by placing a drop of crystals in suspension and allowing the crystals to settle onto the support film. The excess liquid was drained off and a drop of aqueous 2% uranyl acetate was added immediately, in order to prevent drying of the protein crystals. The stain was left on the grid for one minute, after which it was

drained off as thoroughly as possible so as to result in no evident "negative stain" build-up along the edges of the protein crystals.

All specimens were coated with a light but clearly visible layer of evaporated carbon. The purpose of the carbon film is to prevent specimen charging. This step is of particular importance for obtaining good low-angle diffraction patterns of crystalline catalase.

Methods

The radiation "dose" was measured in terms of the current density passing through the specimen support film. The current density was actually measured in the final image plane at a point just below the normal position of the photographic plate. A lithium-drifted silicon detector[1] was used for counting single electrons at rates up to 10^5 counts per second. An aperture of 1.0 mm diameter masked off the detector, and current densities were determined at convenient image magnifications, usually 10,000 to 25,000 times. Current densities were always measured through a clean area of the support film, adjacent to each crystalline specimen being studied.

The radiation-damage end-point for crystalline l-valine and for crystalline adenosine was conveniently taken to be the time at which the diffraction pattern was no longer visible on the fluorescent screen.

---

1. Provided through the courtesy of Mr. F. Goulding, Lawrence Radiation Laboratory, Berkeley.

On the other hand, the diffraction pattern of uranyl-stained catalase does not disappear completely after normal fluxes of electron irradiation. A pattern that might initially extend to Bragg spacings of less than 15 Å will fade down to a resolution of 25 Å to 30 Å. At the same time the relative intensities of the remaining reflections can be altered quite considerably. These changes in the diffraction pattern can be recorded on photographic plates with an electron exposure of only a few per cent of that which is used for the total radiation dose.

The techniques for selected area electron diffraction and for low angle electron diffraction were essentially as described in previous work (13).

Results

The total electron flux at which the diffraction pattern of crystalline l-valine completely disappears has been found in the present work to be $\sim 8 \times 10^{15}$ electrons/cm^2 (at the specimen) at 80 kV and $\sim 2 \times 10^{16}$ electrons/cm^2 at 500 kV. Reciprocity between time for fading and dose rate is shown in Figure 1. The data lie, within experimental error, along a line of slope minus one when the logarithm of fading time is plotted *vs* the logarithm of current density. The total "dose" for complete fading of the diffraction pattern is apparently independent of the intensity (dose rate) of irradiation over the range that has been studied.

The linear energy transfer for 80 kV and for 500 kV electrons was calculated from the relativistic stopping power equation for electrons

(2), using the formulation of Rohrlich and Carlson (27):

$$(1)\quad \frac{-dE}{dx} = .1535\,\frac{\rho}{\beta^2}\,\frac{Z}{A}\,\log\left\{\frac{T^2(T+2)(mc^2)^2}{2I^2} + 1 - \beta^2 + \frac{(T^2/8 - (2T+1)\log 2)}{(T+1)^2}\right\}.$$

In this equation ρ is the density of the specimen; β is the ratio of the electron velocity to the velocity of light; Z is the atomic number and A is the atomic mass (chosen to be 6 and 12 respectively; T is the electron kinetic energy divided by mc^2, which is the electron rest energy; and I is the mean ionization potential. The values computed were 5.5×10^{-2} ev/Å at 80 kV and 2.3×10^{-2} ev/Å at 500 kV, assuming a mean ionization potential of 54.6 ev (the value appropriate to polyethylene) and a density of 1.23. The values of dE/dx are in fact not very sensitive to the exact choice of mean ionization potential within any reasonable range of values. From these values and the electron fluxes mentioned previously it can be further calculated that the energy deposited in crystalline l-valine at the time that structural disorder has been completed is approximately 10^{11} erg/gm, or 10^9 rad. From this figure one can estimate a radiolytic yield of eight molecules damaged per 100 ev absorbed. This value is similar to the ammonia yields for solid amino acids irradiated in vacuum at room temperature, which range from values of approximately 2 to 6 (10).

The diffraction pattern of crystalline adenosine completely disappears after a total electron flux of $\sim 6 \times 10^{16}$ electrons/cm^2, when the accelerating voltage is 80 kV. As is shown in Figure 2, the "dose" for complete fading is again independent of the intensity of irradiation. It is also evident in this figure that crystalline adenosine is 8 to 10 times more resistant to structural disorder occurring as a

result of electron irradiation than is crystalline l-valine. The dose for producing complete disorder of adenosine is calculated from the present data to be approximately 10^{10} rad.

The electron diffraction pattern of uranyl-acetate stained catalase, obtained at 80 kV, does not show any substantial change from the "original"pattern after a radiation flux of only ~ 1×10^{17} electrons/cm^2. However, a flux of 3×10^{18} electrons/cm^2 causes most of the pattern extending beyond a resolution of 25 Å to 30 Å to virtually disappear. Only minor changes occur as a result of an additional radiation "dose" of 6×10^{18} electrons/cm^2. One example of the fading of the diffraction pattern of catalase is illustrated in Figure 3. Each diffraction pattern was recorded with an exposure of 1×10^{16} electrons/cm^2. Detailed features of the diffraction patterns vary somewhat from one crystal to another, depending at least in part upon the specimen tilt, which cannot be controlled accurately on account of warping of the support film. Electron radiation damage also causes relative changes in the intensities of the diffraction orders that remain after a flux of approximately 10^{19} electrons/cm^2. These changes are already noticeable after an irradiation of 10^{18} electrons/cm^2. The relative changes in diffraction intensities are shown in patterns recorded with identical exposure conditions after irradiation by a total dose of 10^{18} electrons/cm^2 and 3×10^{18} electrons/cm^2. As shown in Figure 4, the major change is an increase in the intensity in the $(1,0,\ell)$ reflections relative to the $(2,0,\ell)$ reflections. Other shifts in intensity such as an increase of the (2,0,0) reflection relative to the (2,0,1) and $(2,0,\bar{1})$ reflections are also noticeable.

Theoretical Relationships Between Contrast, Resolution, and Radiation Damage

An image feature can be said to be "resolved" when it is clearly visible from the other features surrounding it. This is manifestly a subjective definition in that the expression "clearly visible" has no quantitative definition. Some image feature that is "clearly visible" on a densitometer tracing might not be so clearly visible on a photographic print. The concept of resolution can depend, among other things, upon the way in which the data are "read" or presented. In the present context we are concerned with the fundamental limitation to resolution that exists because of poor statistics in the measurement and because of the lowest acceptable signal-to-noise ratio regardless of how the data are read or presented.

Image features with low contrast are difficult to "see" at low electron fluxes because the statistical fluctuation of image intensities may exceed the small variation of intensity associated with the intrinsic contrast (1). It is reasonable to assume that the incidence of electrons at the image plane is a random process. If the total number of electrons passing into a given image "point" (picture element) is n, then the statistical fluctuation, or "counting error", is $\sqrt{n}$. It is useful to express this fluctuation in terms of the following parameters: the area of the picture element, d^2; the current density through the object, j; the "integration time" or exposure time, t; and the fraction of the electrons passing through the specimen that actually enter the lens aperture and contribute to the image, f. In terms of these new parameters, $n = fjd^2t$. The statistical fluctuation in particle flux results in a spatially varying "contrast", which is

$\Delta n/n = 1/\sqrt{fjd^2t}$. For a low-contrast image feature to be "resolved", the inherent contrast must exceed the statistical fluctuations by the minimum acceptable signal-to-noise ratio, S/N. This leads to the following inequality

$$(2) \qquad Cd \geq \frac{S/N}{\sqrt{fjt}} \quad .$$

In this equation C denotes the inherent image contrast, which is defined as the difference in image intensity between two points divided by the local average in image intensity. This equation states that the product of resolution and contrast must exceed a certain constant, which is in turn determined by the conditions of measurement (f, j, and t) and by the conditions of analysis (minimum acceptable S/N).

From this equation alone and no further analysis one might erroneously conclude that arbitrarily good resolution could be achieved at arbitrarily low contrast, provided that long enough exposures were recorded at large enough current densities. Such an inference assumes that the dynamic range of the recording medium is sufficient to accommodate the data, and that there are no other factors limiting the resolution. Unfortunately it is not reasonable to use arbitrarily large exposures with biological specimens. Radiation damage can destroy the object to such an extent that an image with statistically well-determined contrast actually may no longer contain meaningful information about the object at the desired resolution.

One useful index of radiation damage is the fraction of bonds broken after a given flux of electrons. This is found in a simple way

from the linear energy transfer, which can be calculated from the stopping power equation, and from the radiolytic yield, which can be measured independently. For a flux of one electron per square Ångstrom, the number of broken bonds is $dE/dx \cdot G$. The linear energy transfer is conveniently expressed in electron volts per Ångstrom. Its value depends upon the accelerating voltage and upon the mass density of the specimen. The radiolytic yield for the processes of concern is designated by the symbol G, and is conveniently expressed in units of "bonds" per electron volt. Dividing by the volume density of bonds, η, gives the fractional bond damage at this particle flux. Multiplying by jt gives the fractional bond damage at any particle flux: $\Delta b/b = dE/dx\ G\ 1/\eta\ jt$.

From the inequality in Equation (2) we find that the integrated flux must be equal to or greater than $(S/N)^2/fC^2d^2$ in order to record an image of some object-feature with contrast C, at a resolution d. From this it follows that a fractional bond damage

$$(3) \qquad \frac{\Delta b}{b} \geq \frac{dE}{dx}\ G\ \frac{1}{\eta}\ \frac{(S/N)^2}{fC^2d^2}$$

will result from the minimum exposure that just permits a resolution of d at a contrast C and a signal-to- (statistical fluctuation) noise ratio, S/N. This equation probably over-estimates by five or ten percent the fractional bond damage at high damage ratios, say larger than 0.5 or 0.75. The reason for this is that the radiolytic yield is defined as a constant, characteristic of the type of molecule and bond. This approximation does not properly take into account the random

occurrence of damaging events in the specimen and the fact that the total damage must reach some saturating value asymptotically rather than linearly.

Representative parametric curves are plotted in Figure 5 for the following choice of constants: $dE/dx = 4.5 \times 10^{-2}$ ev/Å; G = 1 bond per 30 ev; $\eta = 0.2$ bonds/Å^3; S/N = 5 (the value usually quoted for visual perception of structure (28)); f = 1.0. The value taken for η is an approximate value for the total density of all classes of bonds, whereas the value of G is approximately what one expects for scission of the C-N bond in amino acids. The somewhat more consistent approximation of taking $\eta \simeq 0.01$ as the density of C-N bonds for amino acids would result in correspondingly larger estimates of the fractional bond damage, for that class of bonds. This second approximation would assume that the absorbed energy is preferentially channeled to the most labile bond, which is in fact usually the case.

In the case of dark-field electron microscopy the fraction of electrons contributing to the image is very much less than one. Thus while the contrast can be very great in dark-field images (for recent references see for example Dupouy (6), Johnson and Parsons (19), Ottensmeyer (25)), the statistics of measurement for a given exposure are much poorer than in the corresponding bright-field image. As a rough estimate it can be calculated that radiation damage will be twice as great in the dark-field image as in the bright-field image if the contrast is due to Fourier synthesis of the scattered radiation (as in crystal lattice images), while the radiation damage will be nearly equal in the two cases if the contrast is due to truncation of

the Fourier synthesis by the aperture (often referred to as amplitude contrast).

Discussion

Crystalline valine was initially chosen as a specimen for study because it readily forms thin crystals suitable for electron diffraction work (14). Since hydrogen bonds play a major role in the structure of crystalline amino acids, and since other features of structure and of radiation chemistry are partially similar to those of the peptides and proteins it is believed that the results obtained with valine will prove to be roughly comparable to results that might be obtained with an unstained protein. Adenosine was studied since it was a convenient analog for the somewhat more complicated nucleotide-phosphate and nucleic acid structures. Catalase was chosen since it represents one of the highest-resolution examples in the present state-of-the-art for biological specimen preparation. In the best example of the present work the electron diffraction pattern has been seen to extend to less than 9.0 Å (Figure 6).

Measurement of the minimum electron exposure that causes complete fading of a diffraction pattern for a crystalline specimen is of direct significance to understanding the best meaningful resolution that might be obtained in the image. Complete fading of the diffraction pattern would imply that no periodic structure whatever would remain in the image. Even if a few molecules do remain undamaged, there will be no way to recognize them as being unique or to prove from the image data that they represent the original structure. Radiation induced

derivatives of the original structure will also be present in the image, and these will seriously confound the interpretation. In crystalline specimens, and similarly for any specimen that is more than one molecule thick, the overlapping of multiply different radiolytic products will lead to little more than spatial "noise" at resolutions exceeding whatever Bragg reflections may remain.

Although the experimental method used here has been applied for several years in the study of crystalline polymers (20, 32, 37), no data have previously been reported for biological materials. One shortcoming of the method is that it tends to underestimate the dose required to "disorder" or damage a single molecule. One "hit" in an organic-molecular crystal might disorder the entire structure of a unit cell or possibly even the structure of more than one unit cell. Stated another way, the "radiocrystallographic yield" can be larger than the true radiolytic yield. But at least for the purposes of micrographic structure-analysis using crystalline or highly ordered specimens, which has been referred to in the introduction, the "radiocrystallographic yield" is actually the important parameter to know.

The observed differences in the radiation sensitivities of the three specimens reported here requires some explanation. The calculated dose for complete disorder in valine corresponds to approximately thirty electron volts, or one "average" ionizing event, per unit cell. Since there are four molecules in the unit cell (34) this calculation indicates that one ionizing event per every four molecules causes complete disorder of the crystalline structure. The calculated dose

for adenosine is approximately 32 x 10^{-2} ev/$\mathring{A}^3$, or approximately 90 ev/molecule assuming a molecular volume of 286 $\mathring{A}^3$ from the data of Furberg (9). This value indicates that three ionizing events per molecule occur before complete disorder is produced in the crystal. Part of the explanation for the greater resistance to radiation damage in adenosine is probably due to the fact that a substantial fraction of the molecular structure is made up of an heteronuclear, conjugated π-electron system. Because of the delocalizatio of the outer shell valence electrons, structures of this type are relatively stable to single-electron ionizations (26).

The radiation damage reported here for uranyl-acetate stained catalase is almost certainly of a fundamentally different nature from that which occurs in valine and adenosine. The electron exposure for the complete fading effect is approximately three orders of magnitude greater than for valine, and the calculated dose corresponds to approximately two ionizing events per cubic Ångstrom. A reasonable hypothesis concerning the observed radiation damage is that a significant portion of the matter within the unit cell of the structure changes to some more stable configuration as a result of the electron irradiation. This hypothesis would account for the changes in relative intensities of the diffraction maxima that remain after irradiation. Evidently the distribution of matter becomes more disordered as well, since only the lower-resolution Bragg reflections remain. This redistribution of matter probably includes a significant redistribution or aggregation of stain molecules. It is also quite likely that the loss of specimen mass, such as has been reported in the recent work of Williams and

Fisher (39), Stenn and Bahr (31), and in earlier experiments, might contribute to quantitative changes in the relative diffraction intensities.

The electron flux that leads to complete disorder at a given resolution is surely an upper limit to the time-integrated current density, jt, that is reasonable to use in resolving structure at that resolution. The measured values of jt in turn set a lower limit to the product of contrast and resolution, which must be exceeded if meaningful information is to be obtained about the original object structure. It is useful to illustrate this point by some examples of "typical" calculations, using Eq. (2). If one assumes that f = 1.0 (values less than 0.9 would be more precise), S/N = 5 (reasonable for visual perception (28)) and a contrast equal to 0.1, then the best resolution that one might expect, as a result of the limitations of radiation damage, is approximately 50 Å for valine, 20 Å for adenosine, and 1.6 Å for uranyl-acetate stained catalase. For catalase the predicted "best resolution" is in contradiction with the criterion by which the current density was measured, which was that the diffraction pattern would fade to a stable configuration at a resolution of approximately 25 Å to 30 Å. Clearly the lower bound calculated from Equation 2, which is concerned only with the limitations imposed by the statistics of measurement at a predetermined particle flux, is in this case much too low. If a particle flux of 1×10^{17} electrons/cm^2 is used there is no noticeable effect upon the diffraction pattern of catalase to a resolution of at least 17 Å. In this case the best resolution that is compatible with the statistics of measurement is 16 Å, assuming the same parameters as before. This figure is a more reasonable estimate of the "probable best resolution" since it does not contradict the radiation-damage

information derived from the diffraction data.

The results obtained with crystalline catalase also point to another consequence of radiation damage, besides loss of resolution. At a particle flux of 1×10^{19} electrons/cm^2 the diffraction data extend to a resolution of 25 Å to 30 Å, and the image contrast is statistically well determined at this level. However, at this and at even lower resolutions the image structure still is probably of doubtful significance. The reason for concern about the validity of image information at the level of, say, 30 Å to 40 Å is that the intensities of the remaining Bragg reflections have undergone relative changes. This suggests that a redistribution of matter has occurred within the unit cell. If this is in fact the case, then it must be concluded that the presence of periodic structure in the image of a crystalline object is not sufficient evidence that the observed image-features are representative of the original object-structure.

The limitations upon resolution resulting from radiation damage that have been estimated above are examples of what is to be expected for crystalline specimens and other structures of a similar degree of complexity. Single molecules that might be trapped, for example, in a matrix of evaporated carbon or in an inert gas matrix could conceivably tolerate a significantly greater dose of ionizing radiation. This comment supposes that the radiation chemistry of the structure in question is quite simple, as for the example of a single "strand" of polyethylene considered by Stenn and Bahr (30). The products of radiolysis must be immobilized and must be large enough so that they are not displaced significantly into interstitial positions of the

matrix at the time of bond scission. It is not evident that these types of conditions could be achieved for a structure such as a single molecule of a globular protein, or for more complex structures.

It is instructive to answer the question as to why high resolution information can be obtained with crystalline specimens by electron diffraction at much lower levels of illumination than are necessary for direct images. As has been pointed out recently by Breedlove and Trammel (3), the very great spatial redundancy of the object allows one to record as many events in the diffraction pattern as may be necessary, while the fraction of unit cells that experience an ionizing event remains very small. For the purpose of diffraction work a sufficiently large crystal can be very nearly as "good" after a pattern has been obtained as it was before. When a crystal is imaged, however, one forms an image of each identical area of the specimen. Thus for example the same flux of electron irradiation is used if the object contains 10^4 repeating units as when the object is a single free-standing molecule. This analysis suggests that spatial superposition of statistically noisy images might be a possible method for obtaining high resolution images with low amounts of radiation damage. Stated another way the suggestion is to reduce the acceptable S/N in the original record so as to decrease the contrast-resolution product that is compatible with the low radiation density, the value of which is in turn dictated by the limitations of radiation damage. Spatial averaging of micrographs of crystalline and other highly ordered objects has sometimes been used to reduce spatial noise (21,22), but only with images for which the contrast was already statistically well determined.

Other possible methods of minimizing the effect of radiation damage have also been considered. (A) Image intensification is of no direct value, since the problem of image formation at low intensities is basically one of statistics and not of brightness. Furthermore the degree of radiation damage is apparently not dose-rate dependent, as shown by the data in Figures 1 and 2, so that low-intensity microscopy has no inherent advantage. The degree of specimen heating is apparently quite low, in accord with the calculated rise in specimen temperature (30). (B) High voltage electron microscopy does not offer any substantial advantage as regards decreased radiation damage. Figure 7 shows the theoretically expected increase in lifetime of a diffraction pattern for a given current density at the specimen, assuming that there are no dose rate effects. This curve, calculated by the use of Equation 1, shows that the "specimen lifetime" increases by less than a factor of 3 between 100 kV and 1 MeV, after which it again slowly decreases. It is true that not all of the energy lost by the primary beam is actually deposited in a thin specimen, because energetic secondary electrons can escape without losing all of their energy. Nevertheless the ratio of energy lost by the primary beam to the energy deposited in the specimen should not depend strongly upon the accelerating voltage. Thus the relative specimen lifetimes shown in the theoretical curves of Figure 7 should correspond reasonably well to the experimental situation. As has been pointed out by Thomas, et al. (32), what little advantage that the factor of longer specimen lifetime might offer is essentially lost again due to the poorer sensitivity of photographic emulsions and fluorescent screens at the higher voltages! In considering

the use of high voltage electrons the factor of diminishing elastic scattering cross sections must also be taken into consideration.

(C) Low temperature specimen stages designed for operation at liquid helium temperature have been suggested over the years as a possible way to diminish the yield for radiation damage. The primary bond scission would not likely be reduced, but the cage effect of neighboring atoms might keep the specimen structure effectively "intact" at a resolution approaching one Ångstrom. From radiolysis studies it is thought that the loss of hydrogen from polyethylene is not avoided by going to helium temperature (24). Since hydrogen-hydrogen contacts are very important in the structure of organic molecular solids, total specimen disorder might well result, even at very low temperature, at doses that correspond to a high percentage loss of hydrogen. The fading of the diffraction pattern for crystalline polyethylene is reported to be very little affected by low temperature, and this has been interpreted to mean that cross-linking in this material can still proceed at temperatures as low as 20°K, when the radiation dose is great enough to produce large concentrations of alkyl radicals (37). There is some reason to hope, however, that other types of bond damage such as C-N bond scission in polypeptides might have less of a disruptive effect upon the specimen structure at such low temperatures that the (massive) fragments do not have an appreciable thermal motion. In the case of heavy-metal stained specimens one might also expect that low temperatures would inhibit the apparent migration of stain and specimen mass-loss, thereby reducing the spatial disorder that accompanies electron irradiation.

Acknowledgements

The work reported here has been supported by the Division of Biology and Medicine of the U.S. Atomic Energy Commission. Miss Susan Daniels has assisted with specimen preparation and with the radiation damage studies. Dr. Thomas Budinger has contributed to the development of this work by his assistance with the linear energy transfer calculations and by frequent discussions on other aspects of the problems. I thank Professor Gareth Thomas for the opportunity to conduct experiments with the Hitachi 650 kV electron microscope in his laboratory, and Dr. Ted Welton for helpful discussions of radiation damage in biological electron microscopy.

References

1. K. Anderson, J. Sci. Inst. 1, 601 (1968).

2. M.J. Berger and S.M. Seltzer, NASA SP-3012, National Aeronautics and Space Administration, Washington (1964).

3. J.R. Breedlove and G.T. Trammel, Science, In the Press (1970).

4. R.A. Crowther, L.A. Amos, J.T. Finch, D.J. De Rosier, and A. Klug, Nature 226, 421 (1970).

5. D.J. De Rosier and A. Klug, Nature 217, 130 (1968).

6. G. Dupouy, "Electron Microscopy at High Voltages", in Advances in Optical and Electron Microscopy, Vol. 2, R. Barer and V.E. Cosslett, eds., Academic Press (1968).

7. R.P. Ferrier and R.T. Murray, J. Roy. Microsc. Soc. 85, 323 (1966).

8. J. Frank, Optik 30, 171 (1969).

9. S. Furberg, Acta Chem. Scand. 4, 751 (1950).

10. W.M. Garrison, "Radiation Chemistry of Organo-Nitrogen Compounds", in Current Topics in Radiation Research, Vol. 4, M. Ebert and A. Howard, eds., North-Holland Publishing Co. (1968).

11. R.M. Glaeser, 28th Annual Meeting of the Electron Microscopy Society of America, Houston (1970).

12. R.M. Glaeser, T.F. Budinger, P.M. Aebersold and G. Thomas, 7th Intl. Cong. Electron Microscopy, Grenoble (1970).

13. R.M. Glaeser and G. Thomas, Biophys. J. 9, 1073 (1969).

14. R.M. Glaeser, G. Thomas, R. Christensen, and W.G. Brammer, Proceedings 26th Annual Meeting Electron Microscopy Society of America, Claitor Press, New Orleans (1968).

15. R.G. Hart, Science 159, 1464 (1968).

16. R.D. Heidenreich, Fundamentals of Transmission Electron Microscopy, Interscience, New York (1964).

17. W. Hoppe, Acta Cryst., In the Press (1970).

18. W. Hoppe, R. Langer, and F. Thon, Optik 30, 538 (1970).

19. H.M. Johnson and D.F. Parsons, J. Microscopy 90, 199 (1969).

20. K. Kobayashi and K. Sakaoku, Lab. Invest. 14, 1097 (1965).

21. L. Labaw and M.G. Rossmann, J. Ultrastruct. Res. 27, 105 (1969).

22. R. Markham, S. Frey and G.J. Hills, Virology 20, 88 (1963).

23. J.W. Menter, Proc. Roy. Soc. A236, 119 (1956).

24. J.T. Morgan, R. Sheldon, and G.B. Stapleton, RPP/E 13, Rutherford High Energy Laboratory, Chilton Didcot Berkshire, (Oct. 1969).

25. F.P. Ottensmeyer, Biophys. J. 9, 1144 (1969).

26. B. Pullman and A. Pullman, "Quantum Biochemistry", Interscience Publishers, New York (1963), page 277 and page 413.

27. F. Rohrlich and B.C. Carlson, Phys. Rev. 93, 38 (1954).

28. A. Rose, Adv. Electronics 1, 131 (1948).

29. M.G. Rossmann and L.W. Labaw, J. Mol. Biol. 29, 315 (1967).

30. K. Stenn and G.F. Bahr, J. Ultrastruct. Res. 31, 526 (1970).

31. K. Stenn and G.F. Bahr, J. Histochem. Cytochem. 18, 574 (1970).

32. L.E. Thomas, C.J. Humphreys, W.R. Duff, and D.T. Grubb, Radiat. Eff. 3, 89 (1970).

33. F. Thon, Z. Naturforsch. 20a, 154 (1965).

34. M. Tsuboi, T. Takenishi, and Y. Iitaka, Bull. Chem. Soc. Jap. 32, 305 (1959).

35. N. Uyeda, T. Kobayashi, E. Suito, Y. Harada, and M. Watanabe, 7th Intl. Cong. Electron Microscopy, Grenoble (1970).

36. B.K. Vainshtein, V.V. Barynin, and G.V. Gurskaya, Intl. Union of Crystallography, 8th Intl. Cong., Abstracts published in Acta Cryst. A25, Supplement (1969).

37. J.A. Venables and D.C. Bassett, Nature 214, 1107 (1967).

38. B. v. Borries and F. Lenz, Proc. Stockholm Conf. on Electron Microscopy, Stockholm, Alkquist and Wikse11 (1957).

39. R.C. Williams and H.W. Fisher, J. Mol. Biol. 52, 121 (1970).

40. M.G. Wrigley, J. Ultrastr. Res. 24, 454 (1968).

41. K. Yada and T. Hibi, Jap. J. Appl. Phys. 7, 178 (1968).

42. K. Yada and T. Hibi, J. Electromicrosc. 18, 266 (1969).

Figure 1. Radiation damage of crystalline l-valine in the electron microscope, at accelerating voltages of 80 kV and 500 kV. A line with slope minus one indicates a constant-dose relationship for complete fading of the diffraction pattern.

Figure 2. Radiation damage of crystalline adenosine at an accelerating voltage of 80 kV. Data are shown for two independent experiments, and in one of these the radiation sensitivity of valine was measured for comparison.

Figure 3. The diffraction pattern of uranyl-acetate stained catalase is shown (a) before any significant changes have occurred and (b) after irradiating to a degree that no further changes occur. Reflections at Bragg spacings of less than 25 Å to 30 Å are no longer visible after this extensive an irradiation. Data were taken at 75 kV by the three lens method (7) from a field approximately 10 microns in diameter.

Figure 4. Representative changes in the low-order intensities of the electron diffraction pattern of uranyl-stained catalase. The diffraction pattern of the same crystal is shown (a) before irradiation (actual exposure was approximately 10^{16} electrons/cm^2 at the specimen), (b) after irradiation with 10^{18} electrons/cm^2, and (c) after irradiation with 3×10^{18} electrons/cm^2. Data were taken by selected area diffraction from a two micron diameter field at 80 kV.

Figure 5. Representative theoretical curves (cf. Equation 3) showing the relationship between fractional bond damage and resolution for specified values of contrast. Values of the other parameters chosen for these specific curves were $dE/dx = 4.5 \times 10^{-2}$ ev/Å, G = 3 events/100 ev, $\eta = 0.2$, S/N = 5, f = 1.0.

Figure 6. A montage of the diffraction pattern of uranyl acetate stained catalase put together from patterns recorded with different exposure times so that all orders of the diffraction pattern are visible above the diffuse background. The nominal (2,0,18) reflection occurs at a Bragg spacing of 8.2 Å. The relationship between the superficially orthorhombic symmetry of the crystal and the true space group is discussed by Rossmann and Labaw (29).

Figure 7. Theoretical curve showing the change in "radiation damage" at different accelerating voltages. The ordinate, which is measured in units relative to the value at 100 kV, represents the time that is required to deposit a given amount of energy in a given type of specimen when the current density is held constant at all voltages.

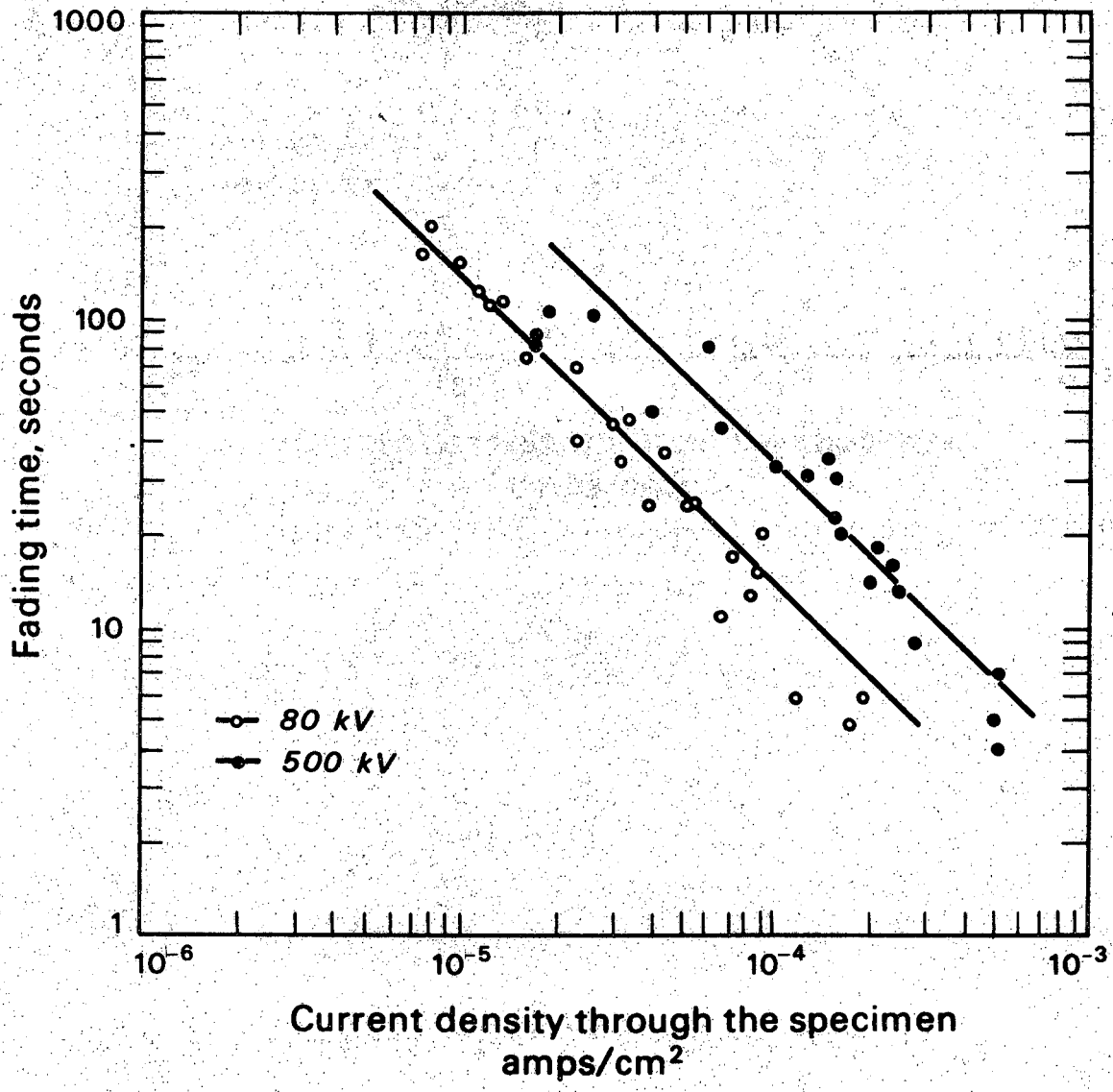
1000
100
10
1
Fading time, seconds
80 kV
500 kV
10^{-6}
10^{-5}
10^{-4}
10^{-3}
Current density through the specimen
amps/cm^2
DBL 703-5623

Fig. 1

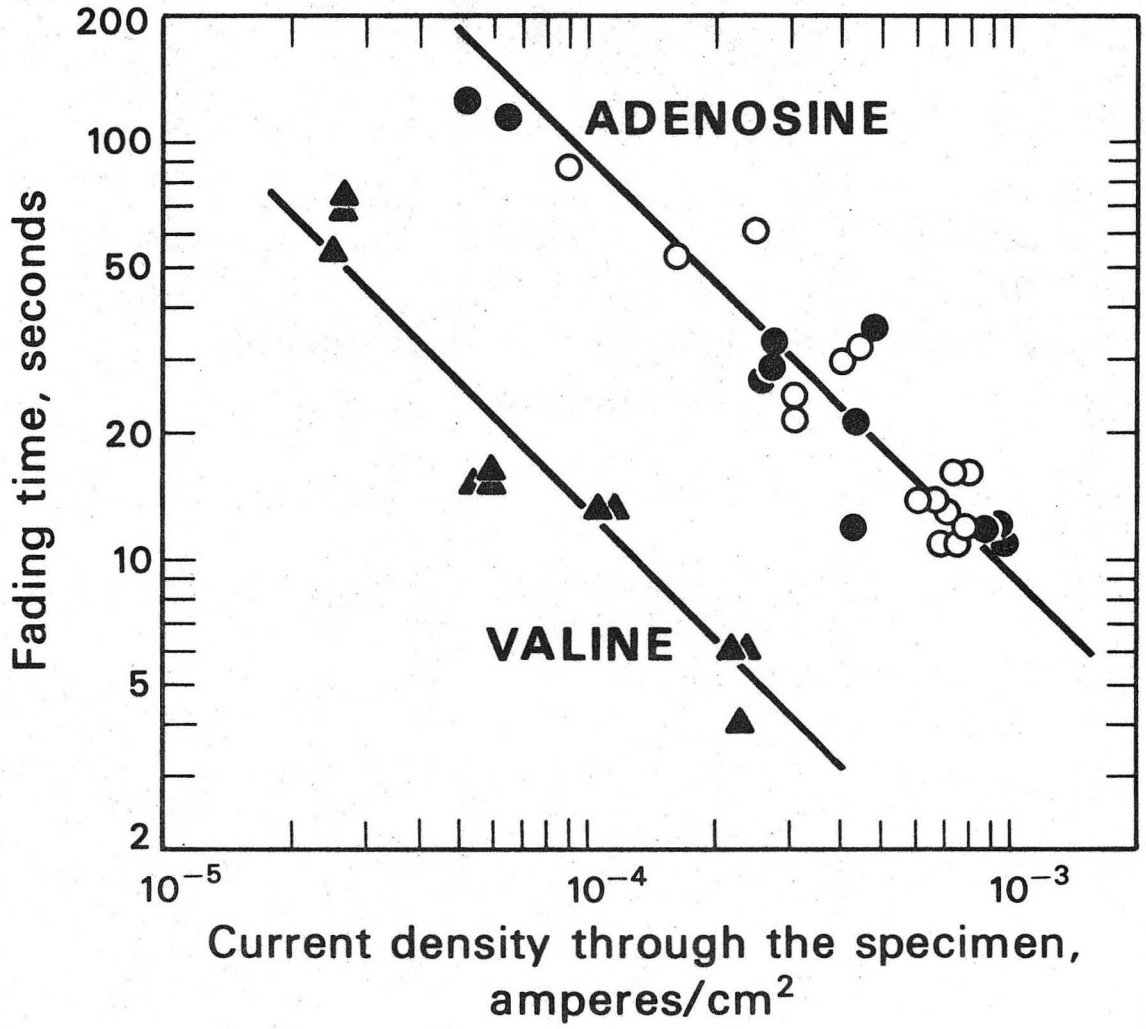

DBL 708 5835

Fig. 2

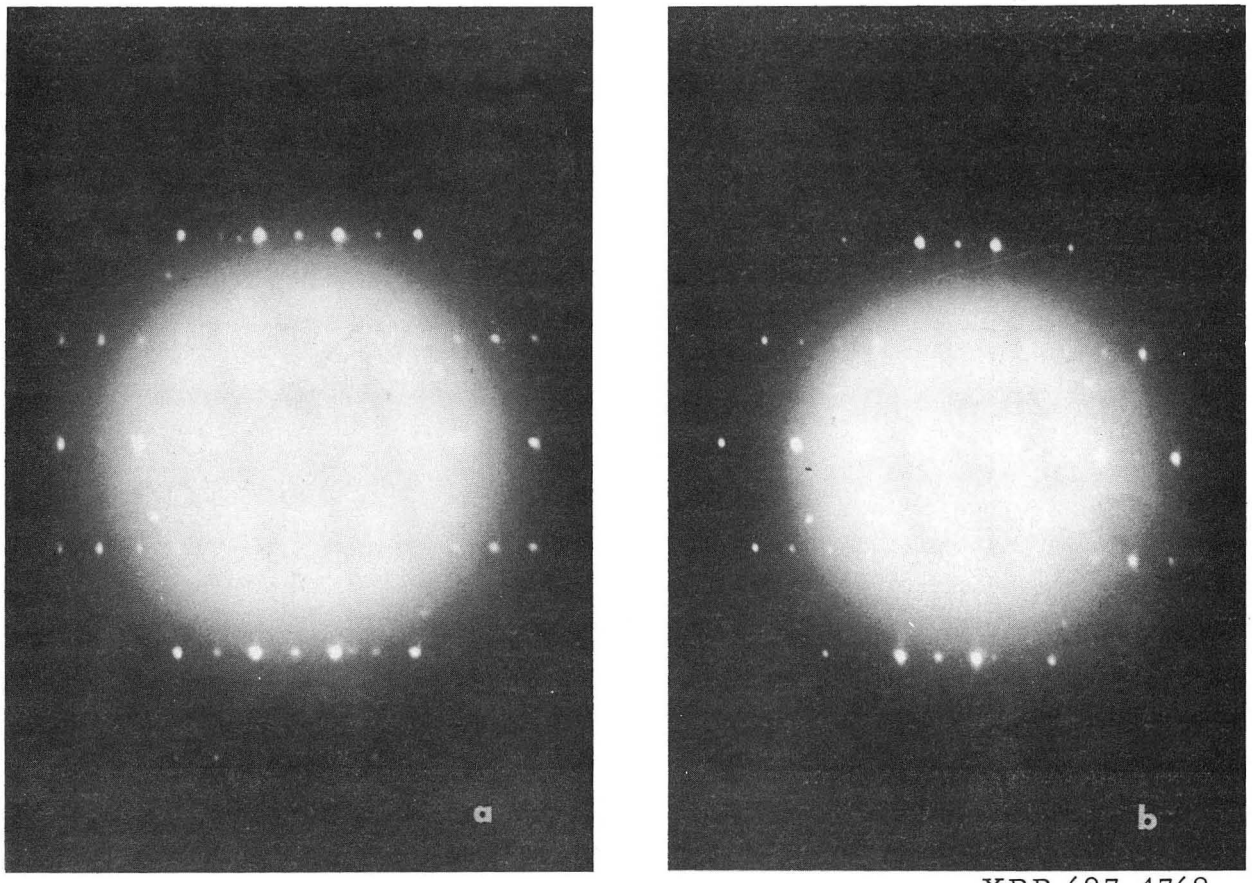

XBB 697-4769

Fig. 3

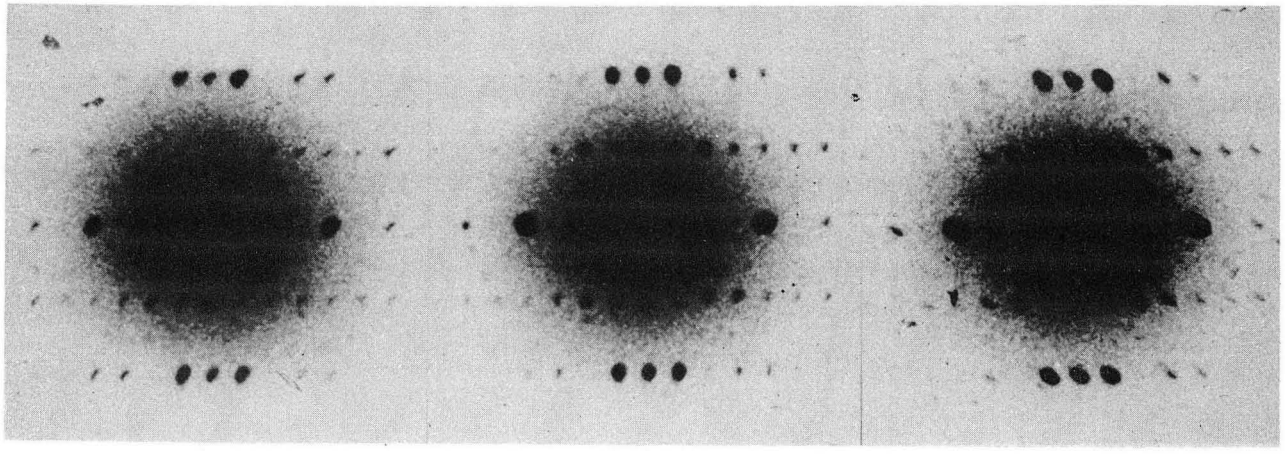

a b c

XBB 708-3625

Fig. 4

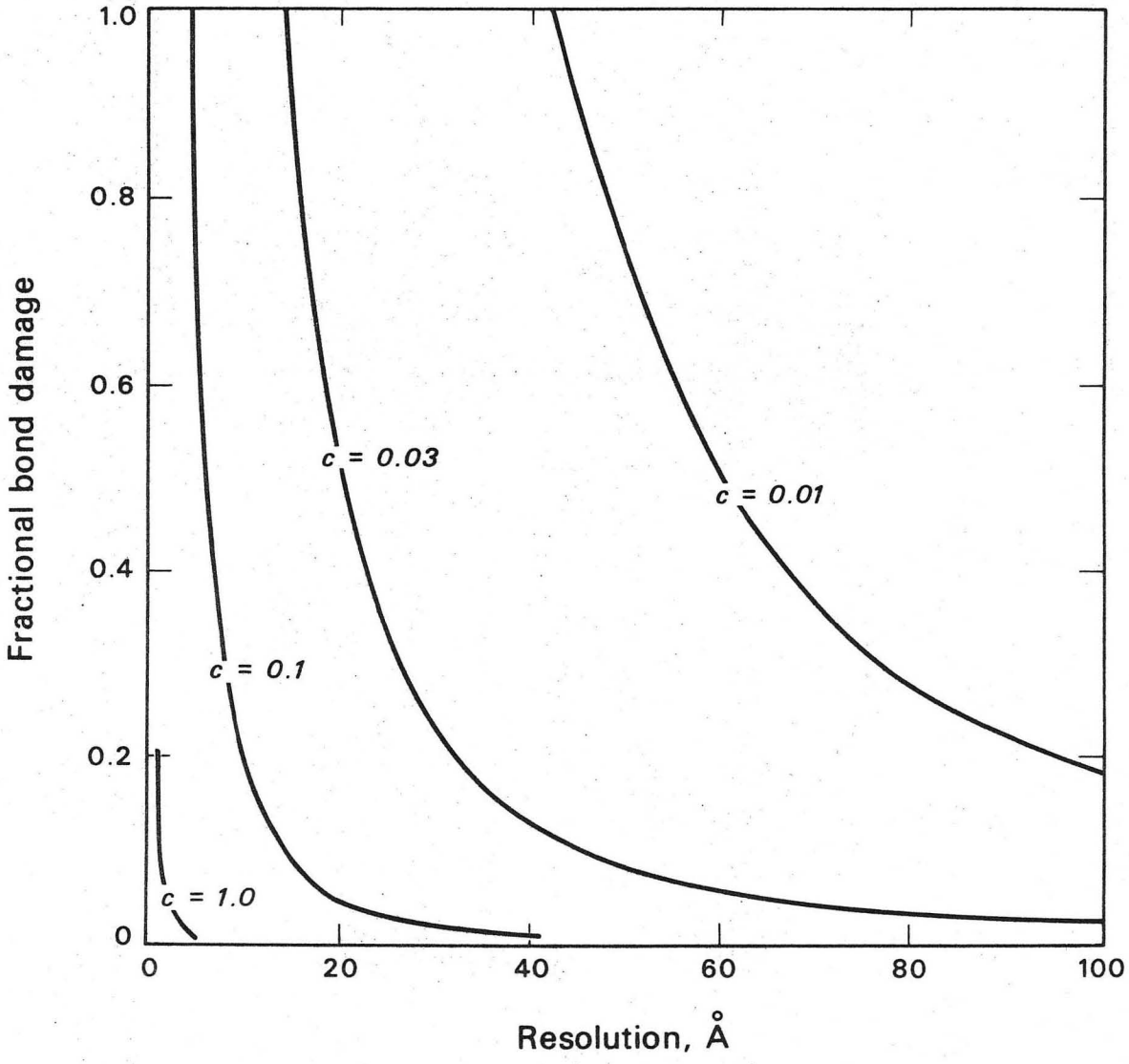

DBL 709 5932

Fig. 5

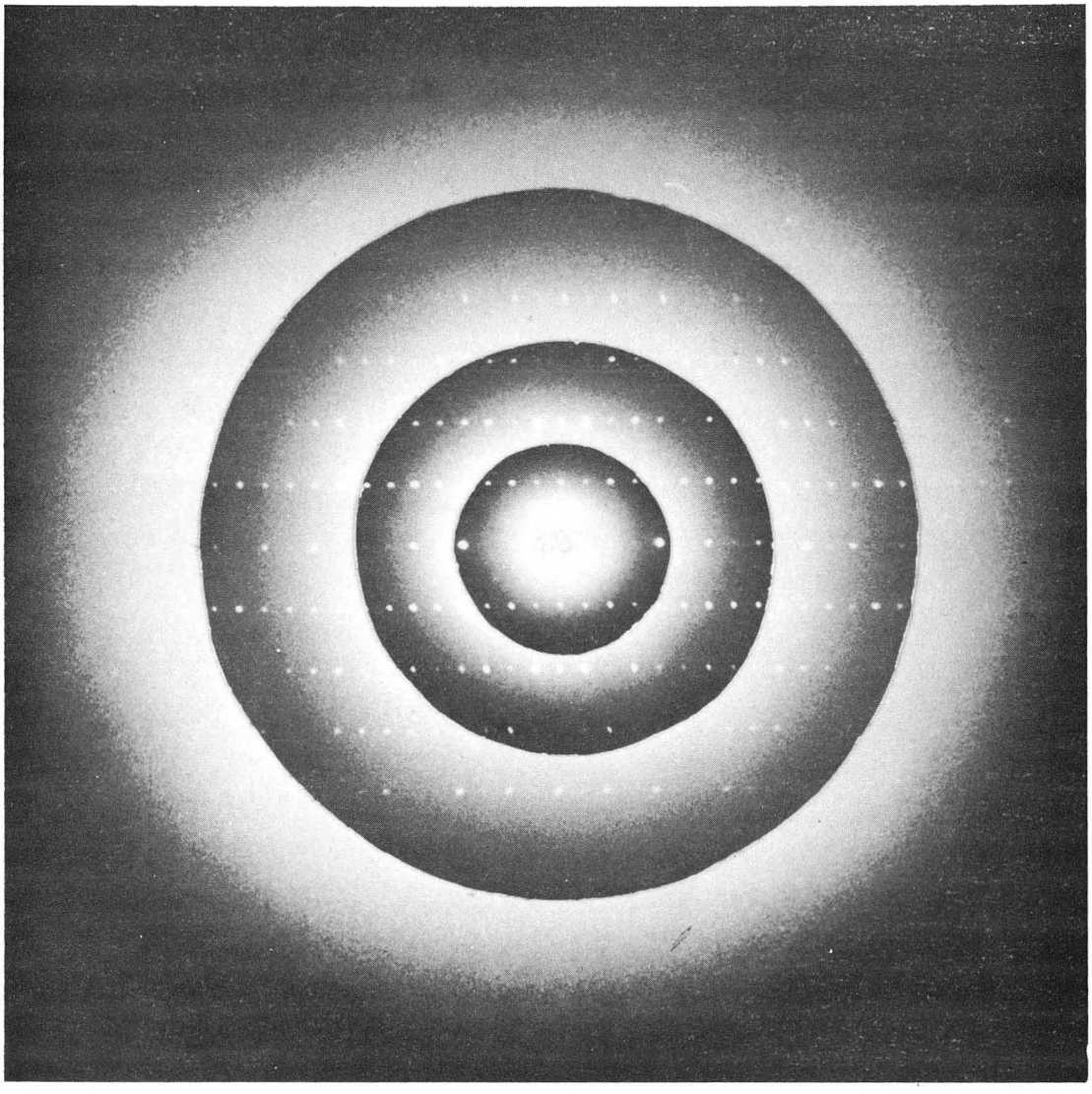

XBB 697-4767

Fig. 6

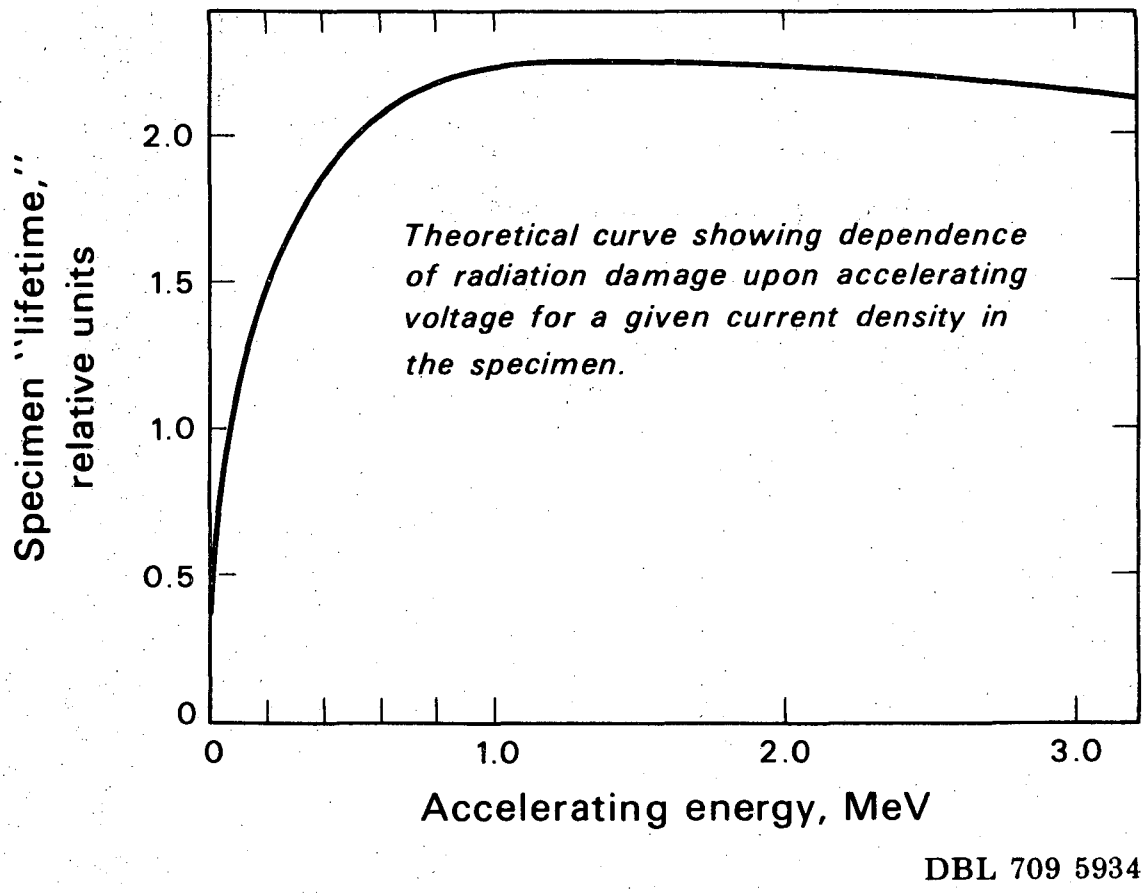

Fig. 7

LEGAL NOTICE

TECHNICAL INFORMATION DIVISION
LAWRENCE RADIATION LABORATORY
UNIVERSITY OF CALIFORNIA
BERKELEY, CALIFORNIA 94720